Electric field gradient and the temperature variation on ^{111}Cd in Re and Zr hcp metal hosts

L. Hermans, M. Rots, J. Claes, G. N. Rao, and R. Coussement
Instituut voor Kern- en Stralingsfysika, K. U. Leuven, B-3030 Leuven, Belgium
(Received 28 July 1980)

The nuclear quadrupole interactions at ^{111}Cd probe nuclei in Re and Zr hosts are measured in the temperature range 4–900 K employing time differential perturbed (γ-γ) angular correlation of the 173–247-keV cascade. Using the known quadrupole moment of the 247-keV state of ^{111}Cd, the electric field gradient (EFG) at 293 K for ^{111}Cd*Re* $= 1.60\times10^{17}$ V/cm^2 and for ^{111}Cd*Zr* $= 0.79\times10^{17}$ V/cm^2. Both metallurgically prepared and implanted sources were used. The temperature variation of the EFG for ^{111}Cd*Re* is quite small and is about 12% over the temperature range 4–860 K. Since the sign of the EFG is known from (β-γ) angular correlation measurements reported earlier, we are able to obtain the electronic part precisely. The electronic part is about 2.1 times the lattice part and is essentially constant over the temperature range studied showing that the entire temperature variation comes from the lattice part. For ^{111}Cd*Zr* the electronic part is about 1.9 times the lattice part if we assume that the sign of the electronic contribution is opposite to the sign of the lattice part. The EFG is highly temperature dependent and changes by about 57% over 4–890 K. For this system also, the temperature dependence is neither given by the linear T dependence nor by the $T^{3/2}$ law. The results are discussed in the light of the systematic trends and the currently available semiempirical and theoretical models.

I. INTRODUCTION

The large number of hyperfine-interaction experiments reported during the recent years on the electric field gradients (EFG) and the associated temperature variation on various probe nuclei in hcp metals have led to the identification of many interesting systematic trends. This in turn generated considerable theoretical interest to develop appropriate theories leading to a better understanding of the different mechanisms involved on the origin of the EFG's.[1] The observed EFG is ordinarily separated into the lattice and the electronic contributions. The lattice contributions are usually calculated using the Das and Pomerantz[2] formula after taking account of the appropriate antishielding factors. The electronic part is traditionally obtained by subtracting the lattice contributions from the measured EFG. First-principles calculation of the electronic contributions to the EFG are difficult because one would require the wave functions for all the occupied states of the electrons. It is well recognized that the electronic contributions are quite significant and have large temperature dependence. In spite of the admittedly complex nature of the electronic contributions coming from the core, valence, and the conduction electrons, a fairly simple correlation has been observed for most of the measured systems where the electronic contributions were found to be 2–3 times the lattice part and are of opposite sign.[3] This important observation qualitatively signifies that the lattice is essentially responsible for the origin of the EFG and the electron cloud is distorted by the lattice to result in an amplified EFG at the nuclear site. Recent experiments show that there are many exceptions to this rule.[4,5] Many cases were reported where the signs of eq_{el} and eq_{latt} are not of opposite sign. Another important result is that very large enhancements of the order of up to about 50 were observed for some selected transition-metal hosts and for some probe ions belonging to the second half of the transition series.[6-8] This may possibly be due to the large d density of states resulting in strong localized EFG contributions. The local contributions to EFG's seem to differ from the behavior of the local d moments with which we are familiar from the neutron scattering and hyperfine field measurements on transition-metal impurities in ferromagnetic hosts. For ferromagnetic hosts the magnitudes of the d moments on the impurities follow well-defined trends depending on the electronic configuration of the impurity and have a maximum value when the d shell is about half-full and minimum values close to zero when the d shell is empty or fully occupied. In contrast very large local contributions to the EFG are observed only for certain transition-metal probes in specific transition-metal hosts.

Though the electronic contributions to the temperature variation of the EFG are expected to be quite complex, almost all the experimental data seem to follow a simple $T^{3/2}$ dependence with few exceptions. There are many attempts to explain the observed systematics on temperature dependence with varying degrees of success. Even though most of the models dealing with the temperature variation can explain the observed $T^{3/2}$ dependence, they often fail to give an estimate of the magnitude of the EFG.

It is quite clear that more experimental data would be very helpful to check the validity of the already established systematic trends, to look for possible new surprises, and to test the theoretical predictions. In this paper we report our experimental results on the EFG's and their temperature variation for ^{111}Cd*Re* and ^{111}Cd*Zr* systems. The experimental data are discussed in the light of the various systematic trends and with the semiempirical and theoretical models wherever applicable. In particular the data on ^{111}Cd*Zr* are compared with the values obtained from the detailed calculations using the conduction-electron charge shift model recently suggested by Bodenstedt and Perscheid.[9]

II. EXPERIMENTAL

A. Source and sample preparation

For the present measurements we make use of the well known 173–247 keV (γ-γ) cascade in the decay of ^{111}In (2.8 *d*) to the levels of ^{111}Cd. The intermediate state of 247 keV in ^{111}Cd with a half-life of 84 nsec is well suited for the time differential perturbed angular correlation (TDPAC) experiments.

(*a*) ^{111}Cd*Re*. The parent ^{111}In (2.8 *d*) activity was implanted into a Re single crystal as well as into polycrystalline Re foils at an approximate dose of 1.5×10^{13} ions/cm^2 with an energy of 75 keV. The implanted unannealed sources and also the sources obtained by implantation followed by annealing at 400 °C resulted in a somewhat attenuated amplitude with the same main quadrupole interaction frequency. This may possibly be due to the existence of a component, owing to the damaged sites produced during implantation. Since the quality of the spectra improved enormously when we annealed the source at 800 °C for about 10–12 h, it may be inferred that the damaged sites produced during the implantation process become annealed during annealing. Therefore, for the present measurements, the samples were annealed at 800 °C for about 12–14 h in a high-purity argon atmosphere and were cooled gradually. The quadrupole interaction frequency and the variation with temperature obtained with the single crystal and the polycrystalline samples are in good agreement. The samples prepared by implantation on single crystals gave zero distribution in the EFG's whereas the spectra obtained with the polycrystalline samples showed a small distribution in the EFG's. The nominal maximum impurity concentration is less than 150 ppm as implanted but the actual concentrations are likely to be much smaller because of the heat treatment given to the samples.

(*b*) ^{111}Cd*Zr*. The sources were prepared by both metallurgical and implantation methods. The ^{111}In (2.8 *d*) activity was prepared by an (α, 2*n*) reaction on a high-purity silver foil of 0.025 mm thickness with an α energy of 25 MeV at the UCL (Université Catholique de Louvain) cyclotron. The typical doses are about 15 μA h. The foils were allowed to cool for approximately two days so that most of the ^{109}In (4 h) impurity activity decays. A small part of the silver foil (1 mm $\times$ 1 mm) was cut from the most active part of the Ag foil and was melted with high-purity zirconium in an arc furnace in argon atmosphere. The resulting shining metal ball was annelaed at 750 °C for about 12–14 h in argon atmosphere, cooled gradually, and was used for the perturbed angular correlation (PAC) experiments. The second procedure adapted for the sample preparation was to evaporate a drop of active indium chloride in high-purity zirconium, melting in an arc furnace in argon atmosphere followed by annealing at 800 °C for about 12 h.

The sources were also prepared by implanting ^{111}In activity into high-purity Zr foils at a dose of 4×10^{13} ions/cm^2 at an energy of 75 keV. Unannealed implanted sources resulted in a large distribution of the EFG's. Good quality sources were obtained only when we melted and annealed the sources after implantation. The quality of the spectra obtained is almost identical for all the above methods used for the preparation of the samples. The sources prepared with the commercially available high-purity Zr foils resulted in a distribution in the EFG's and this was apparent from the large attenuation of the amplitude of the oscillation observed as a function of time. This may possibly be due to the impurities in the commercially available Zr foils which are stated to be of 99.7% purity. Zirconium is known to be highly sensitive even to small quantities of Hf impurities.[10] Good-quality spectra were obtained only when we used high-purity Zr ingot for the sample preparation. All the samples prepared in the present experiments gave a consistent and reproducible quadrupole interaction frequency. Even for the commerical Zr foils, though the distribution in the EFG's is considerable, the main interaction frequency remains unchanged. The solubility data of In in Zr are not available. The electronegativity difference of In compared to Zr is +0.3 and the atomic radii of Zr and In are of the same order of magnitude. Therefore In*Zr* system satisfies the Hume-Rothery limits of solid solubility (atomic radius ± 15% and electronegativity ± 0.4). In view of this one may infer that, at least for the concentrations of In used in the present experiments, In is soluble in Zr. Also,

for the good quality and the reproducibility of the spectra obtained for the variety of samples we had prepared using different methods followed by different heat treatments, one can say that the probe nuclei are occupying reproducible unique sites and are probably substitutional. The impurity concentrations are less than 1 ppm for the metallurgically prepared samples using carrier free $InCl_3$, about 100 ppm for the samples prepared using ^{111}InAg foil and about 340 ppm for the implanted sources.

B. Fitting procedure

The general expression for the PAC function may be written[11]

$$W(\vec{K}_1, \vec{K}_2, t) = \sum_{k_1 k_2, N_1 N_2} \frac{A_{k_1}(\gamma_1) A_{k_2}(\gamma_2)}{[(2k_1+1)(2k_2+1)]^{1/2}} G_{k_1 k_2}^{N_1 N_2}(t)\, Y_{k_1}^{N_1 *}(\Phi_1 \phi_1) Y_{k_2}^{N_2}(\Phi_2 \phi_2). \quad (1)$$

The angles (Φ_1, ϕ_1) and (Φ_2, ϕ_2) are the polar and azimuthal angles of the directions $\vec{K}_1$ and $\vec{K}_2$ along which the γ_1 and γ_2 are observed with respect to arbitrary choosen axis of quantization. The spherical harmonics Y_k's give the angular part of the angular correlation. The so-called perturbation factor $G_{k_1 k_2}^{N_1 N_2}(t)$ contains the essential information on the interaction between the moment of the nucleus with the external field.

For the case of single-crystal samples with axially symmetric EFG, the perturbation factor

$$G_{k_1 k_2}^{NN}(t) = \sum_{n=0}^{n_{max}} S_{nN}^{k_1 k_2} \cos n\omega_0 t. \quad (2)$$

However, for polycrystalline samples with axially symmetric EFG, the perturbation factor

$$G_{kk}(t) = \sum_n S_{kn} \cos n\omega_0 t. \quad (3)$$

For half-integer spins, the frequency ω_0 is related to the quadrupole coupling constant ν_Q by

$$\omega_0 = \frac{3\Pi}{I(2I-1)} \nu_Q \quad \text{and} \quad \nu_Q = \frac{e^2 qQ}{h}, \quad (4)$$

where Q is the nuclear quadrupole moment and eq is the largest component of the EFG tensor in the principal axis system.

A conventional 4-detector setup with NaI(Tl) scintillation detectors and a PDP-8 on-line computer were used for data acquisition. Two detectors A and B were used to generate the "start" pulses and the other two detectors C and D to obtain "stop" pulses. The chance coincidences were subtracted from each of the time spectra and the $R(t)$ values calculated:

$$R(t) = \frac{\mathfrak{C}_{AC}(\pi, t)\mathfrak{C}_{BD}(\pi, t)}{\mathfrak{C}_{AD}(\pi/2, t)\mathfrak{C}_{BC}(\pi/2, t)} - 1, \quad (5)$$

where $\mathfrak{C}_{AC}(\pi, t)$, $\mathfrak{C}_{BD}(\pi, t)$ and $\mathfrak{C}_{AD}(\pi/2, t)$, $\mathfrak{C}_{BC}(\pi/2, t)$ are the true coincidences in a small time window Δt when the angles between the detectors are π and $\pi/2$, respectively. This experimental arrangement considerably reduces the difficulties in centering the source, unequal efficiencies of the detectors, etc. at least to the first order. For both ^{111}Cd*Re* single-crystal experiments and ^{111}Cd*Zr* polycrystalline sample experiments the function $R(t)$ given by Eq. (5) may be expressed in terms of $\cos n\omega_0 t$ (where $n = 0, 1, 2, 3$ for the 247-keV level, $I = \frac{5}{2}$ of ^{111}Cd) multiplied by the appropriate amplitudes [see Eqs. (2) and (3)]. Therefore the data were fitted to the equation

$$R(t) = \sum_{n=0}^{3} S_n e^{-(1/2)(n\omega_0 \sigma t)^2} \cos n\omega_0 t. \quad (6)$$

The exponent terms allow the possible distribution in the EFG's assuming that the distribution is Gaussian. The width of the distribution $(2\sigma/\omega_0)$ was used to decide the quality of the sources particularly for the case of zirconium host. For the case of ^{111}Cd*Zr* also, the coefficients S_n were allowed as free parameters during the fitting procedure to take account of the possible texture effects due to incomplete randomness of the crystallites. For our ^{111}Cd*Re* single-crystal experiments, the fitted amplitudes (S_n) obtained are in agreement with the expected values for the orientation of the single crystal used in the experiments. The time resolution of the detectors is quite small compared to the time period corresponding to the quadrupole interaction frequencies, and therefore the corrections due to the finite time resolution of the detectors were not included in the data analysis. The periodicity of the spin-rotation spectra obtained for ^{111}Cd*Re* clearly show that the system is axially symmetric. For ^{111}Cd*Zr*, because of the low quadrupole interaction frequency involved, we could observe only one but well-defined oscillation. Earlier reported experiments on ^{181}Ta*Zr* showed that $\eta \sim 0$ within the experimental errors.[12] These results coupled to our present experiments indicate that $\eta \sim 0$ for ^{111}Cd*Zr* also. The fitting procedure followed for the final data analysis included S_n, ω_0, and σ as free parameters for both ^{111}Cd*Re* and ^{111}Cd*Zr*.

III. RESULTS AND DISCUSSION

A. EFG at ^{111}Cd in Re host

The quadrupole interaction frequency

$$\nu_Q(^{111}\mathrm{Cd}Re) = -29.73(14)\ \mathrm{MHz}\ \text{at}\ 293\ \mathrm{K},$$

where

$$\nu_Q = \frac{e^2Qq}{h} = \left(\frac{10}{3\pi}\right)\omega_0 .$$

The sign was obtained from the $(\beta\text{-}\gamma)$ angular correlation measurements of Raghavan *et al.*[3] Our value is in agreement with the value of 29.2(6) reported by the above authors. Taking the quadrupole moment of the 247-keV level of ^{111}Cd as $+0.77(12)b$ (Ref. 13) which is in agreement with the recent measured values of $+0.83(13)b$ (Ref. 14) and $+0.80(7)b$ (Ref. 15), the electric field gradient at ^{111}Cd probe nuclei in the Re matrix is 1.6×10^{17} V/cm^2 at 293 K. The observed nuclear quadrupole spin-precession spectra are given in Fig. 1 where we have plotted $R(t)$ vs t. The single-crystal experiments were carried out with the c axis parallel to the plane of the detectors. The amplitude of the spin-precession pattern is unattenuated even up to about four time periods showing that all the probe nuclei are occupying unique sites and practically no distribution in the EFG's $(2\sigma/\omega_0 = 0)$. The data were also fitted using (a) the asymmetry parameter η and (b) an additional component having a different quadrupole interaction frequency. For both of them the quality of the fits did not improve and the fitted parameters show that η as well as the intensity of the second component are zero within the statistical uncertainties. The electronegativity difference of In compared to Re is -0.2 and the atomic radius of In is larger by 21% compared to that of Re. These values may be compared with the Hume-Rothery limits[16] for solid solubility (atomic radius ±15% and electronegativity ±0.4). Since our samples were prepared by implantation, modified Hume-Rothery limits[17] suggested for metastable substitutional solutions are expected to be applicable where the solubility limits are (a) atomic radius, -15% to $+40\%$ of the host radius and (b) the electronegativity within ±0.7 of that of the host atoms. The scheme recently proposed by Miedema and co-workers[18] also show that the In is likely to be soluble in the Re host. In view of these points, one may infer that for the concentrations of In used in the present experiments, In is soluble in the Re host. The quality of the spin-rotation spectra observed in our experiments is good. The fitted amplitudes correspond to the expected values for the orientation of the single crystal used. Also, the quadrupole interaction frequency is in agreement with

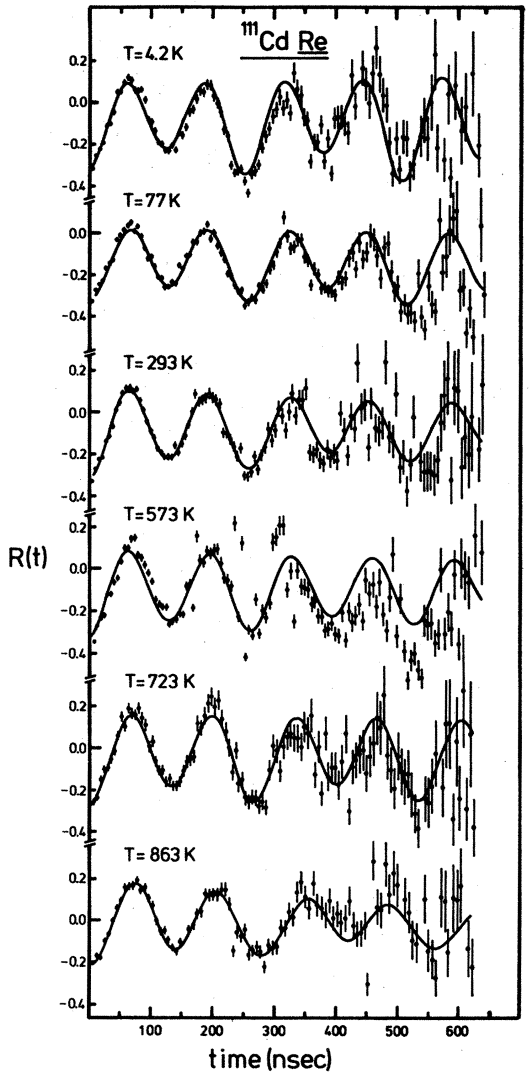

FIG. 1. Time dependence of $R(t)$ for the nuclear quadrupole interaction of the 247-keV level of ^{111}Cd in Re single crystal at different temperatures.

the results of Raghavan *et al.*,[3] where they prepared the samples by implanting ^{111}Ag in Re single crystal. From all these facts we infer that we are sampling the EFG on ^{111}Cd probe nuclei occupying random substitutional positions in a Re host.

The electric field gradient (eq) is traditionally written as

$$eq = eq_{\mathrm{ion}} + eq_{\mathrm{el}}, \qquad eq_{\mathrm{ion}} = eq_{\mathrm{latt}}(1-\gamma_\infty), \tag{7}$$

where eq_{ion} is the contribution to the EFG from the ions in the lattice. The electronic contribution eq_{el} is obtained by subtracting the ionic part from the experimental value. The lattice contribution is calculated from the Das and Pomerantz formula

$$eq_{\text{latt}} = \left(\frac{ez}{a^3}\right)\left[0.0065 - 4.3584\left(\frac{c}{a} - 1.633\right)\right]. \quad (8)$$

Using the known lattice parameters of Re and the Sternheimer antishielding factor $(1-\gamma_\infty) = 34.35$ and for $Z = 7$, we obtain $eq_{\text{ion}} = 1.48\times10^{17}$ V/cm^2 and $eq_{\text{el}} = 3.08\times10^{17}$ V/cm^2.

The data obtained at different temperatures are given in Table I. The antishielding factor $(1-\gamma_\infty)$ was taken from the recent calculations of Das and his group[19] using Hartree-Fock nonrelativistic wave functions. The values of the lattice parameters of Re were obtained from the work of Finkel *et al.*[20] in the temperature range 77–300 K. The high-temperature values were obtained by normalizing the values quoted by Pearson[21] to the room-temperature values of Finkel *et al.* As observed earlier the electronic contribution is about 2.1 times the lattice contribution and is of opposite sign confirming the universal correlation.

One of the recent surprises is that some of the impurities belonging to the second half of the transition-metal impurities in transition-metal hosts experience very large EFG's sometimes with an enhancement factor of up to 50.[6-8] Re is a transition-metal host and the measured EFG's on different probes are tabulated in Table II to look for such large enhancements. The values of α range from 1 to 2 even for transition elements of the second half such as Fe, Os, and Ir showing that all the data are in good agreement with the universal correlation and the localized contributions are negligible.

B. Temperature variation of the EFG for ^{111}Cd in Re host

The measured values of the quadrupole interaction frequencies are plotted against T in Fig. 2 and against $T^{3/2}$ in Fig. 3. It is clear that the data can be fitted to neither linear T nor $T^{3/2}$ dependence. All the data presented in Table I were taken with a single source. The c/a ratio for the Re metal is 1.6139 at room temperature, which is considerably less than the ideal ratio of 1.633 and the c/a value reduces considerably as we increase the temperature. From the variation of c/a value with temperature, one would expect a large variation in the EFG as a function of temperature. The observed temperature variation is only about 12% over the temperature range studied and this can be explained by the expected temperature dependence of the lattice contributions alone showing that no measurable temperature dependence is contributed from the electronic part even though the electronic part is about 2.1 times the lattice contribution. We believe that the small scattering in the values of eq_{el} is probably due to the errors in the values of eq_{latt} resulting from the large uncertainties in the lattice parameters as a function of temperature. Normally the electronic part is expected to have significant contribution the net temperature dependence of the EFG. Further $\delta eq_{\text{el}}/\delta eq_{\text{latt}}$ could be temperature dependent. From the *ab initio* calculations of Das and his group,[22] one can say that the different contributions from the electrons such as $\delta q_{pw\text{-}pw}$, $\delta q_{pw\text{-core}}$, δq_{core} are of such sign and magnitude that most of the contributions get cancelled resulting in very marginal net change in $eq_{\text{el}}(T)$. The interesting feature is that this gets cancelled over the entire temperature range studied. It will be worthwhile to compare our results with the work of Butz and Potzel[23] who reported the temperature variation of the EFG on ^{181}Ta in Re. The observed a variation of about 1.3% in EFG and about 3.5% in eq_{el} over a temperature range 1.2 to 450 K. However, it should be added that one would expect that ^{181}Ta being a transition-metal probe may behave differently from the normal-metal probe such as ^{111}Cd. It appears that the small temperature dependence seems to be the property of the Re host. More data on other probe nuclei in an Re host would be helpful to check this trend.

TABLE I. The observed quadrupole interaction frequency at ^{111}Cd probe nuclei in Re at different temperatures. eq_{expt} is the electric field gradient at ^{111}Cd in Re and eq_{ion} and eq_{el} are the ionic and the electronic contributions as discussed in the text.

T (K)	ν_Q (MHz)	eq_{expt} in 10^{17} V/cm^2	eq_{ion} in 10^{17} V/cm^2	eq_{el} in 10^{17} V/cm^2
4.2	30.51(15)	−1.639		
77	30.08(15)	−1.616	1.420	−3.036
293	29.73(15)	−1.597	1.484	−3.081
573	29.38(15)	−1.578	1.538	−3.116
723	28.16(14)	−1.513	1.584	−3.097
863	26.84(13)	−1.442	1.594	−3.036

TABLE II. The measured electric field gradients on different probe nuclei in Re host. All the data were taken from Ref. 1 except as noted.

Probe	Elect. conf.	eq_{expt} in 10^{17} V/cm^2	Probe $(1-\gamma_\infty)$	$eq_{ion}=(1-\gamma_\infty)\,eq_{latt}$ in 10^{17} V/cm^2	$\alpha=\frac{eq_{expt}}{eq_{ion}}$
^{57}Fe	$3d^6 4s^2$	−0.50	10.14	0.435	−1.2
^{111}Cd[a]	$4d^{10}5s^2$	−1.597	34.35	1.474	−1.1
^{181}Ta	$5d^3 6s^2$	−5.52	62	2.66	−2.1
^{187}Re	$5d^5 6s^2$	−4.7	51	2.19	−2.2
^{189}Os	$5d^6 6s^2$	−2.9	47	2.02	−1.4
^{197}Hg	$5d^{10}6s^2$	−2.82	61.2	2.63	−1.1
^{189}Ir[b]	$5d^7 6s^2$	−3.6	44	2.0	−1.8

[a] Present measurements.
[b] D. W. Murray *et al.*, Hyperfine Interact. 7, 481 (1980).

C. EFG at ^{111}Cd in Zr host

The quadrupole interaction frequency

$$\nu_Q(^{111}\mathrm{Cd}Zr) = 14.76(7)\ \mathrm{MHz}\ \text{at}\ 293\ \mathrm{K},$$

which is in approximate agreement with the value of $\nu_Q = 14.1(2)$ MHz recently reported by Kaufmann.[24] Taking the quadrupole moment of the 247-keV state in ^{111}Cd is $= +0.77b$, this results in an electric field gradient of $\pm 0.79 \times 10^{17}$ V/cm^2. Using the known lattice parameters of Zr,[25] and the antishielding factor $(1-\gamma_\infty) = 34.35$ and for $Z = 4$, we obtain the ionic contribution $eq_{ion} = 1.07 \times 10^{17}$ V/cm^2. In the present experiments the sign of the quadrupole interaction is not measured and therefore the electronic contribution eq_{el} is -0.28×10^{17} V/cm^2 or 1.86×10^{17} V/cm^2 depending on whether the quadrupole interaction is positive or negative. The observed spin-rotation spectra are displayed in Fig. 4 and the results are given in Table III. Typical values obtained for the width of the distribution $(2\sigma/\omega_0) = 0.08$.

From the data presented in Table IV it is seen that for different probes in zirconium host, the values of α vary in the range 0.7 to 10. Zirconium seems to behave in a fashion somewhat similar to that of scandium because, for the data available, a large enhancement factor for the EFG was observed for only one impurity, i.e., Fe which is a transition metal belonging to the second half.

D. Temperature dependence of the EFG at ^{111}Cd in Zr host

The observed quadrupole interaction frequency (ν_Q) is plotted versus T in Fig. 5 and versus $T^{3/2}$ in Fig. 6. It is clear that the temperature dependence is neither given by a linear T nor $T^{3/2}$ dependence. For this system, the temperature variation is large and the electronic contributions

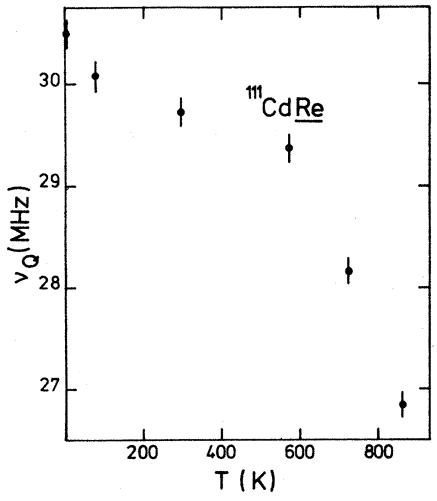

FIG. 2. Quadrupole interaction frequency (ν_Q) vs T for ^{111}Cd*Re*.

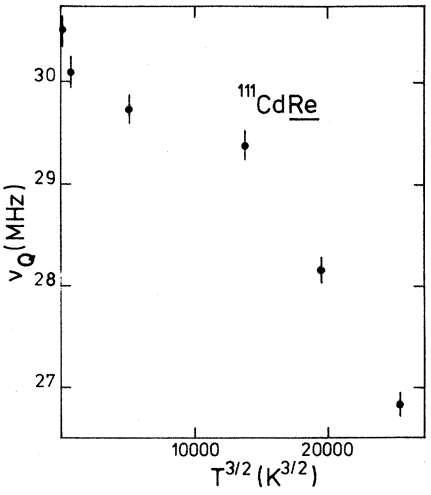

FIG. 3. Quadrupole interaction frequency (ν_Q) vs $T^{3/2}$ for Cd*Re*.

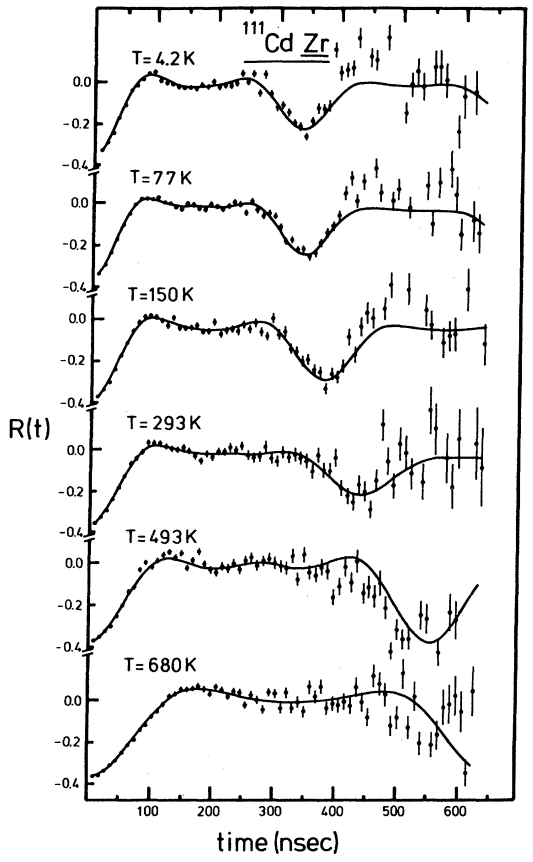

FIG. 4. Time dependence of $R(t)$ for the nuclear quadrupole interaction of the 247-keV level of ^{111}Cd in polycrystalline Zr at different temperatures.

to the temperature dependence are very significant. The EFG changes by about 57% in the temperature range 4–890 K. The eq_{ion} changes by about 13% and the electronic part by about 35% if we assume that the quadrupole interaction is negative. The ^{111}CdZr and ^{111}CdRe systems behave quite different in their temperature dependence of the EFG. While the electronic contributions for the temperature dependence are negligible for ^{111}CdRe, they contribute very significantly for the ^{111}CdZr system.

IV. COMPARISONS WITH CONDUCTION-ELECTRON CHARGE SHIFT MODEL

Bodenstedt and Perscheid recently suggested the conduction-electron charge shift model[9] which is successful in explaining approximately the observed EFG and the temperature variation. Close agreement with the experimental values was obtained for Zn (Ref. 9) and for ^{57}Fe in Zn, Cd, and Ti hosts,[26] whereas the calculations gave a somewhat lower value compared to the observed EFG for ^{57}FeZr (Ref. 27) possibly due to the strong local contributions from the d electrons. In this model, the EFG can be calculated easily because we need only the elastic constants of the host matrix at different temperatures and no explicit knowledge of the electron wave functions is required.

The conduction electrons are assumed to fill the space between the ions and this distribution is approximately split into separate charge clouds so that point ion summation may be carried out. The EFG in a pure metal is given by[9]

$$eq_{\text{pure metal}} = [eq_{\text{ion}} - \tfrac{1}{6} eq_{\text{hp}}(1+\delta) - \tfrac{1}{6} eq_{\text{el}}(1-\delta)](1-\gamma_\infty), \quad (9)$$

where $(1-\gamma_\infty)$ is the antishielding factor and eq_{ion}, eq_{hp}, and eq_{el} are the field gradients at the nuclear site from the positive-ion cores and from the electron charge clouds in the hexagonal plane and from the charge clouds in between the hexagonal planes.

Using the reported measurements of C_{ij} for Zr,[28] S_{ij}'s are calculated and are given in Table V. These values are used to calculate the charge

TABLE III. The observed quadrupole interaction frequency (QIF) at ^{111}Cd in Zr at different temperatures. eq_{expt} is the electric field gradient at ^{111}Cd in Zr. eq_{ion} and eq_{el} are the ionic and the electronic contributions as detailed in the text.

T (K)	ν_Q (MHz)	eq_{expt} in 10^{17} V/cm^2	eq_{ion} in 10^{17} V/cm^2	+QIF eq_{el} in 10^{17} V/cm^2	−QIF eq_{el} in 10^{17} V/cm^2
4.2	19.26(10)	±1.035	1.086	−0.051	−2.121
77	18.90(9)	±1.015	1.088	−0.073	−2.103
150	17.29(9)	±0.929	1.082	−0.153	−2.011
293	14.76(7)	±0.793	1.069	−0.276	−1.862
493	11.76(6)	±0.632	1.041	−0.409	−1.673
680	9.84(5)	±0.529	1.002	−0.473	−1.531
890	8.29(4)	±0.445	0.945	−0.500	−1.390

TABLE IV. The measured electric field gradients on different probes in Zr host. All the data were taken from Ref. 1 except as noted.

Probe	Elect. conf.	eq_{expt} in 10^{17} V/cm^2	Probe $(1-\gamma_\infty)$	$eq_{\text{ion}}=(1-\gamma_\infty)eq_{\text{latt}}$ in 10^{17} V/cm^2	$\alpha=\frac{eq_{\text{expt}}}{eq_{\text{ion}}}$
Fe[a]	$3d^6 4s^2$	±3.17	10.14	0.32	±9.9
Zr	$4d^2 5s^2$	±3.68	29.09	0.90	±4.1
Mo	$4d^5 5s^1$	±1.9	22.43	0.69	±2.8
Cd[b]	$4d^{10} 5s^2$	±0.793	34.35	1.07	±0.7
Ta	$5d^3 6s^2$	±5.15	62	1.92	±2.7

[a] H. C. Verma *et al.*, unpublished.
[b] Present measurements.

shifts δ for different Z_{eff},

$$\delta=\left[\frac{c}{a}-\left(\frac{8}{3}\right)^{1/2}\right]\Big/\left[Z_{\text{eff}}^2 e^2\left(\frac{8}{3}\right)^{1/2}\right] \times \frac{36\epsilon_0 a^4}{\frac{1}{6}(S_{11}+S_{12}-2S_{13})+S_{33}-S_{13}}. \quad (10)$$

For the pure host matrix, the EFG at the host ion of effective charge $Z_{\text{eff}}e$ is

$$eq^P(Z_{\text{eff}})=\frac{4Z_{\text{eff}}e}{4\pi\epsilon_0 a^3} \times\left((1+\delta)-(1-\delta)\frac{\frac{1}{2}(c/a)^2-\frac{1}{3}}{\left[\frac{1}{4}(c/a)^2+\frac{1}{3}\right]^{5/2}}\right), \quad (11)$$

and the EFG at the impurity ion is given by

$$eq^{\text{probe}}(Z'_{\text{eff}})=[eq^{\text{bare}}_{\text{ion}}-eq^P(Z_{\text{eff}})+eq^P(Z'_{\text{eff}})](1-\gamma_\infty^{\text{probe}}). \quad (12)$$

The calculated EFG values for different values of Z_{eff} and Z'_{eff} and the experimental values are given in Table VI. Part of the screening may take place within the ion cores and therefore precise values of Z_{eff} and Z'_{eff} are not known. The variation of the antishielding factor $(1-\gamma_\infty)$ for different values of Z'_{eff} are not reported in the literature and therefore we use the value of $(1-\gamma_\infty)=34.35$ reported[19] for Cd^{2+}. The EFG calculated from the conduction-electron charge shift model is in approximate agreement with the experimental value. For example for $Z_{\text{eff}}=4$ and $Z'_{\text{eff}}=1.5$ the calculated value of EFG $=-1.3\times10^{+17}$ V/cm^2 compared to the experimental value of $0.80\times10^{+17}$ V/cm^2.

The conduction-electron charge shift model in the present form does not take account of the local contributions. Cadmium being a normal-metal probe is not expected to have any strong local contribution and therefore one would expect that

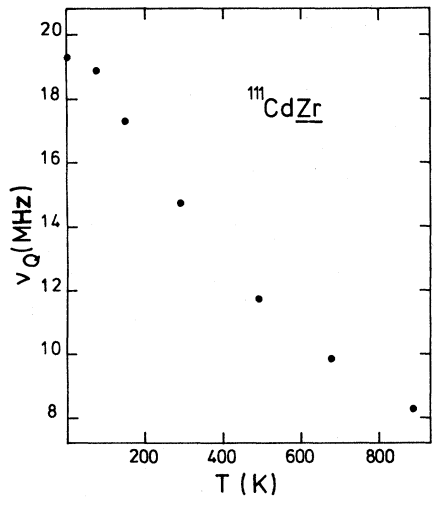

FIG. 5. Quadrupole interaction frequency (ν_Q) vs T for $^{111}CdZr$.

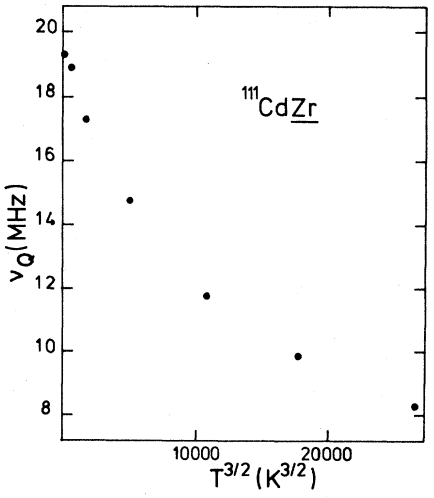

FIG. 6. Quadrupole interaction frequency (ν_Q) vs $T^{3/2}$ for $^{111}CdZr$.

TABLE V. Compliance constants of zirconium in units of 10^{-13} cm^2/dyne.

T (K)	S_{11}	S_{12}	S_{13}	S_{33}
4.2	8.408	−2.756	−2.117	7.294
77	8.672	−2.902	−2.167	7.426
123	8.891	−3.056	−2.222	7.567
298	10.123	−4.042	−2.409	7.977
467	11.728	−5.395	−2.600	8.412
566	12.889	−6.378	−2.740	8.713

this model would be applicable for ^{111}CdZr. Even though the calculated value is about 50% larger than the experimental value, in the opinion of the authors this should be considered reasonable in view of the crude approximations involved.

Temperature variation of the EFG

The temperature variation mostly comes from (a) the changes in the elastic constants and the lattice parameters with temperature and from (b) the vibrations of the ions. From the known elastic constants and the lattice parameters as a function of temperature, the EFG's are calculated for different values of Z_{eff} and Z'_{eff} and are also given in Table VI. The model predicts a change of about 29% for $Z_{\text{eff}} = 4$ and $Z'_{\text{eff}} = 1.5$ compared to an observed change of about 57% over a temperature range 4–890 K. In this model,[9] the contributions from the lattice vibrations are significant and are from (a) the oscillations of the conduction-electron charge clouds and (b) the anisotropic vibrations. These contributions are not included in the present calculations because of the nonavailability of reliable data on the mean square displacements $\langle x_i^2 \rangle$ of the probe ions in the respective host matrices.

V. CONCLUSIONS

The measured values of the electric field gradients for ^{111}Cd$Re = 1.6 \times 10^{17}$ V/cm^2 and for ^{111}Cd$Zr = 0.79 \times 10^{17}$ V/cm^2 at 293 K. The EFG on ^{111}CdRe is weakly temperature dependent and changes by about 12% over 4–860 K. Even though the electronic part is about 2.1 times the lattice part, the electronic part does not contribute to the temperature dependence and the entire temperature variation comes from the lattice only. The EFG on ^{111}CdZr is highly temperature dependent and changes by about 57% over 4–890 K. For ^{111}CdZr system, the electronic part contributes very significantly for the temperature-dependent part. Both the systems are unusual in the sense that the temperature-dependent part is not given by the linear T or linear $T^{3/2}$ dependence. The conduction-electron charge shift model recently suggested by Bodenstedt and Perscheid seems to offer a simple and easy method to estimate the zero order EFG. When reliable data on the elastic constants of Re become available, it would be interesting to compare the predictions of this model with the EFG and its temperature variation for ^{111}CdRe also.

ACKNOWLEDGMENTS

We are grateful to Dr. Michel Cogneau of the Nuclear Chemistry division and to the cyclotron staff at the Université Catholique de Louvain for the numerous cyclotron irradiations. Our thanks are also due to Renaat Vanautgaerden for preparing the implanted sources and Willy Scholaert for the metallurgically prepared sources. This work was supported by the I.I.K.W.

TABLE VI. Calculated values of the electric field gradients for ^{111}CdZr system using the conduction-electron charge shift model of Bodenstedt and Perscheid. Experimental values are given at the bottom of the table.

$\frac{Z_{\text{eff}}}{Z}$	Z'_{eff}	Temperature (K) 4.2	77	150	293	493	680	890
0.750	1.00	−1.553	−1.533	−1.488	−1.422	−1.317	−1.204	−1.069
	1.50	−1.801	−1.777	−1.724	−1.647	−1.526	−1.394	−1.236
	2.00	−2.048	−2.021	−1.961	−1.873	−1.734	−1.584	−1.403
0.875	1.00	−1.368	−1.352	−1.314	−1.260	−1.172	−1.077	−0.962
	1.50	−1.562	−1.544	−1.500	−1.437	−1.337	−1.228	−1.096
	2.00	−1.756	−1.735	−1.687	−1.615	−1.502	−1.378	−1.229
1.000	1.00	−1.250	−1.237	−1.204	−1.157	−1.081	−0.998	−0.898
	1.50	−1.410	−1.394	−1.358	−1.304	−1.218	−1.124	−1.010
	2.00	−1.569	−1.552	−1.511	−1.451	−1.355	−1.249	−1.121
Expt. values		±1.035	±1.015	±0.929	±0.793	±0.632	±0.529	±0.445

[1]E. N. Kaufmann and R. J. Vianden, Rev. Mod. Phys. 51, 161 (1979).
[2]T. P. Das and M. Pomerantz, Phys. Rev. 123, 2070 (1961).
[3]P. Raghavan, E. N. Kaufmann, R. S. Raghavan, E. J. Ansaldo, and R. A. Naumann, Phys. Rev. B 13, 2835 (1976).
[4]K. Krien, M. Forker, F. Reuschenbach, and R. Trozinski, Hyperfine Interact. 7, 19 (1979).
[5]H. Ernst, E. Hagn, E. Zech, and G. Eska, Phys. Rev. B 19, 4460 (1979).
[6]M. Forker and K. Krusch, Phys. Rev. B 21, 2090 (1980).
[7]K. Krusch and M. Forker, Z. Phys. B 37, 225 (1980).
[8]R. Vianden, J. Kotthaus, and P. Winand, Z. Phys. B 37, 221 (1980).
[9]E. F. Bodenstedt and B. Perscheid, Hyperfine Interact. 5, 291 (1978).
[10]R. L. Rasera, T. Butz, A. Vasquez, H. Ernst, G. K. Shenoy, B. D. Dunlop, R. C. Reno, and G. Schmidt, J. Phys. F 8, 1579 (1978).
[11]H. Frauenfelder and R. M. Steffen, in *Alpha, Beta, and Gamma Ray Spectroscopy*, edited by K. Siegbahn (North-Holland, Amsterdam, 1965), Vol. 2, p. 997.
[12]E. N. Kaufmann, Phys. Rev. B 8, 1382 (1973).
[13]R. S. Raghavan, P. Raghavan, and J. M. Friedt, Phys. Rev. Lett. 30, 10 (1973); P. Raghavan, E. N. Kaufmann, R. S. Raghavan, E. J. Ansaldo, and R. A. Naumann, Phys. Rev. B 13, 2835 (1976).
[14]P. Herzog, K. Freitag, M. Reuschenbach, and H. Walitzki, Z. Phys. A 294, 13 (1980).
[15]H. Ernst, Thesis, Technische Universität, München, 1979 (unpublished).
[16]W. Hume-Rothery, R. E. Smallman, and C. W. Haworth, *The Structure of Metals and Alloys* (Institute of Metals, London, 1969).
[17]D. K. Sood, Phys. Lett. 68A, 469 (1978).
[18]A. R. Miedama, J. Less-Common Met. 32, 117 (1973); A. R. Miedema, R. Boom, and F. R. de Boer, *ibid.* 41, 283 (1975); R. Boom, F. R. de Boer, and A. R. Miedema, *ibid.* 46, 271 (1976).
[19]T. P. Das, Phys. Rev. B (in press).
[20]V. A. Finkel, M. I. Palatnik, and G. P. Kovtun, Fiz. Met. Metalloved. 32, 212 (1971).
[21]W. B. Pearson, *Handbook of Lattice Spacings and Structures of Metals and Alloys—2* (Pergamon, New York, 1967), p. 1199.
[22]M. D. Thompson, P. C. Pattnaik, and T. P. Das, Phys. Rev. B 18, 5402 (1978).
[23]T. Butz and W. Potzel, Hyperfine Interact. 1, 157 (1975).
[24]E. N. Kaufmann, Fifth International Conference on Hyperfine Interactions, Berlin, 1980. Abstracts of Invited and Contributed Papers, C16-II.
[25]J. Goldak, L. T. Lloyd, and C. S. Barrett, Phys. Rev. 144, 478 (1966).
[26]H. C. Verma and G. N. Rao, Phys. Lett. (in press).
[27]H. C. Verma, J. Chappert, and G. N. Rao, Hyperfine Interact. (in press).
[28]E. S. Fisher and C. J. Renken, Phys. Rev. 135A, 482 (1964).